ISBN: 978-3-95450-231-8 ISSN: 2673-5490 doi: 10.18429/JACoW-IPAC2023-MOPM034

SHUNT IMPEDANCE CALCULATIONS FOR AN IN-VACUUM UNDULATOR AT PETRA IV

F. Quetscher*, E. Gjonaj, H. De Gersem, Technische Universität Darmstadt, Darmstadt, Germany

Abstract

A new in-vacuum undulator (IVU) with varying gap width is being developed for the new X-Ray source, PETRA IV at DESY. Its electromagnetic properties need to be investigated. These include, especially, the losses in the flexible taper transitions between the beam pipes and in the magnet array, as well as the impact of the IVU's impedance on beam stability. To assess the impedance of the structure, we employ numerical simulations. The challenges lie in the large size of the IVU, the wide frequency range due to the short bunch length, the highly resonant response of the system, and in the complex geometry of the structure. In a first step, wakefield simulations are carried out using CST Studio Suite. Subsequently, the shunt impedances are calculated by eigenmode simulations with the CST Studio Suite and a specialized in-house frequency domain impedance solver.

INTRODUCTION

High-brightness light sources play a crucial role in various applications, such as three-dimensional X-ray microscopy, examining biological, chemical, and physical processes at length scales from atomic dimensions to millimetres and time scales below nanoseconds. The upcoming PETRA IV X-Ray source at DESY will extend the range of radiation wavelengths to nanometre scales [1]. A new in-vacuum undulator (IVU) will be used for this purpose.

The electromagnetic properties of the IVU are crucial for ensuring its optimal performance. In particular, the longitudinal shunt impedances of higher-order modes (HOMs) are of interest due to an observed longitudinal instability at the predecessor facility, PETRA III [1]. Simulating the behaviour of the IVU is challenging, given its large size (≈4.6 m) and the high frequencies of interest, up to around 30 GHz [1]. Furthermore, the IVU's geometric details, such as the small gap width (1 − 5 mm), magnet assemblies, and coolant pipes add to the complexity of the simulation.

To estimate the beam and shunt impedances, three different solvers are employed: the wakefield solver and the eigenmode solver, both from the CST Studio Suite, as well as an in-house impedance solver using the Finite Element Method in the frequency domain. Each simulation technique has its own strengths and limitations. By utilising all three we can compare and evaluate the accuracy of the results.

MODEL DESCRIPTION

The model of the IVU considered in the simulations is shown in Fig. 1. It consists of a parallel plate magnet array covered by thin nickel-coated copper foils. The gap width of the IVU is adjustable, however, it is fixed to 5 mm in the simulations. At the entry and exit sections of the IVU, flexible taper structures made of copper are used to ensure an smooth transition between the beam pipe and magnet array. The tank is made of stainless steel, whereas the magnet array is supported by a number of aluminium blocks.

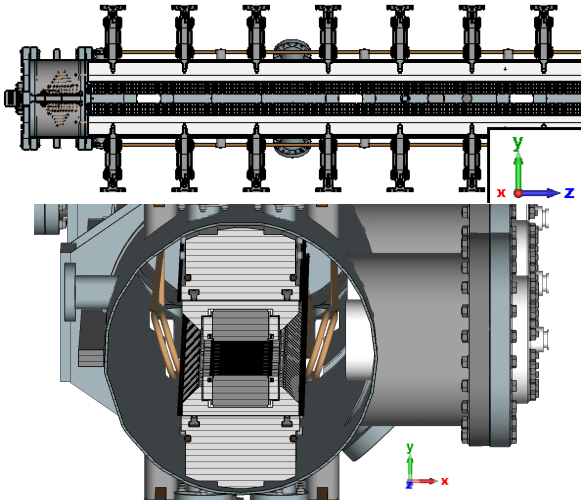

Figure 1: Top: side view of half of the IVU. Bottom: front view.

The middle section has a shape akin to a ridge waveguide [2]. This shape determines the pattern of the ground mode and the first HOMs. At frequencies up to 3 GHz, there is no coupling of any modes to a beam propagating on-axis due to the shape of the geometry and due to the symmetry in the xz-plane. Consequently, the corresponding shunt impedances are zero in this case. However, the impedance of the structure is revealed when the beam is displaced in the y-direction. This is the case considered in the following.

SIMULATION PROCEDURE

In order to reduce computational costs, the model is slightly simplified. Small mechanical features like screws are neglected. Furthermore, the magnet array is assumed to be homogeneous. The flexible taper is approximated with a linear taper. Neglecting the coolant pipes, small asymmetries in the entry and exit sections, and mirroring the vacuum pumps creates a symmetry in the yz-plane. Furthermore, copper and aluminium are modelled as perfect electric conductors (PEC). This is justified since the dominant part of the losses occurs in the tank.

Each of the utilised solvers presents distinct advantages and inherent limitations. The wakefield solver is based on the Finite Integration Technique (FIT) in the time domain. Thus, the solver has minimal memory demands. However, its draw-

* frederik.quetscher@tu-darmstadt.de

ISBN: 978-3-95450-231-8 ISSN: 2673-5490 doi: 10.18429/JACoW-IPAC2023-MOPM034

backs include poor geometry approximation due to the hexahedral mesh. In addition, long simulation times are needed to obtain a sufficient frequency resolution for highly resonant structures. Both the eigenmode and impedance solvers benefit from shorter simulation times and superior geometry approximation due to tetrahedral meshes. Nonetheless, their achievable accuracy and simulated frequency range are constrained by high memory demand.

The shunt impedances are obtained by postprocessing the field simulation data. For the eigenmode solver, the field patterns and quality factors are obtained individually for each eigenmode. The voltage V_i exerted on a point charge traversing the IVU chamber by eigenmode i can be computed by integrating along the beam's path, as

$$V_i = \int_a^b E_{z,i}(z) e^{j\omega_i z/c_0} dz, \tag{1}$$

where a and b are the positions of entrance and exit of the chamber, respectively, and c_0 denotes the speed of light. Utilising this voltage, the longitudinal shunt impedance $R_{s,i}$ can be calculated as

$$R_{s,i} = \frac{|V_i|^2 Q_i}{2 W_i \omega_i}, \tag{2}$$

with W_i being the total energy stored in the field, Q_i the Q-factor, and ω_i the resonance frequency of the eigenmode [3].

The wakefield solver and the impedance solver provide the total beam coupling impedance. In order to extract shunt impedances from the beam impedance, the computed impedances are expressed in a pole-residual representation

$$Z(\sigma) = d + \sigma e + \sum_{k=1}^{K} \frac{c_k}{\sigma - p_k}. \tag{3}$$

This representation is obtained by employing the vector fitting technique [4], which is implemented in the scikit-rf Python library. The pole-residual decomposition enables the construction of an equivalent circuit [5] allowing for the extraction of shunt impedances and facilitating a comprehensive comparison between the solvers.

RESULTS

Figure 2 displays the impedances simulated using the wakefield and impedance solvers, respectively. The earlier uses $18.5 \cdot 10^6$ hexahedrons (85 cells per wavelength (cpw) at 1GHz) with an integrated wake length of 1km. The latter uses of 255k volume elements (10cpw at 1.5 GHz) utilising 3rd order basis functions. In both cases, in order to excite the eigenmodes, the beam is displaced from the symmetry axis by 0.5 mm in y-direction.

The resonance frequencies computed by the two solvers show reasonable agreement, particularly at lower frequencies. However, there are important differences between the curves. The impedance obtained from the wakefield solver exhibits a frequency-independent component of $\approx 10\Omega$, which is absent in the impedance solver's result. Furthermore, there is an unphysical DC component in the impedance

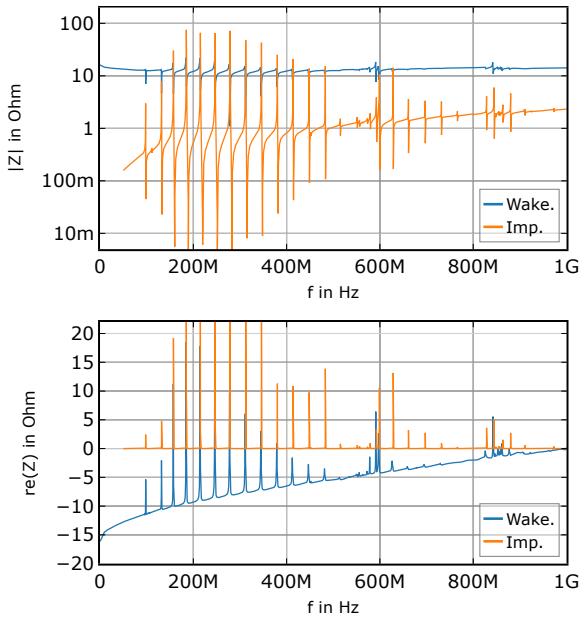

Figure 2: Beam impedances simulated with the wakefield and the impedance solver, respectively.

of the wakefield solver. Additionally, a negative real part of the impedance implies an energy gain by the beam, thus violating energy conservation in a passive structure. Both effects do not diminish significantly with higher wakelengths or finer meshes.

For the shunt impedance analysis, first, the eigenmode solver is employed together with Eq. (2). The solver uses 155k tetrahedrons (10cpw at 1.5 GHz) and employs 2nd order basis functions. It uses less mesh cells than the impedance solver, as it does not need a fine mesh around the beam.

Figure 3 shows the shunt impedances and R/Q-s obtained with the three solvers. The results of the eigenmode and impedance solvers are considered accurate within the limits of numerical error. The wakefield solver's results are inaccurate and are included for the sake of completeness only.

As seen in this figure, the results from the two frequency domain solvers agree well below 500 MHz. The characteristic quantities of the dominant modes within this frequency range, as calculated by the eigenmode and impedance solver, can be found in Table 1.

At higher frequencies, the deviation between the solvers is much more pronounced. This includes a band of modes in the range of 600 MHz to 800 MHz where the shunt impedances differ by factors in the range of 1.5 to 8. Nonetheless, these modes still follow a similar pattern.

DISCUSSION

The wakefield solver exhibits the lowest accuracy. This could be due to either the geometric approximation using the hexahedral mesh or the beam boundary condition. A convergence study, in which the mesh was varied from $1.5 \cdot 10^6$ to $250 \cdot 10^6$ mesh cells, did not reveal any significant change

ISBN: 978-3-95450-231-8 ISSN: 2673-5490 doi: 10.18429/JACoW-IPAC2023-MOPM034

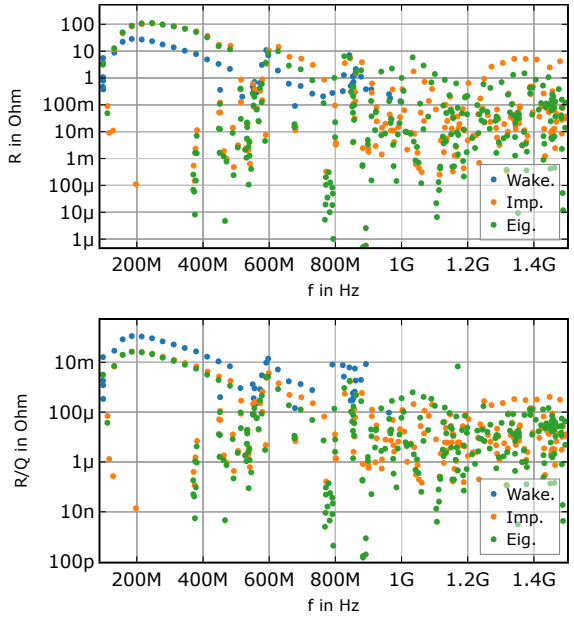

Figure 3: Longitudinal shunt impedances calculated by the three solvers.

Table 1: Resonance frequencies, shunt impedances and Q-factors of the dominant modes calculates by the impedance and eigenmode solvers, respectively.

#	f_0/MHz		R_s/Ω		Q	
	Imp.	Eig.	Imp.	Eig.	Imp.	Eig.
1	97.81	97.32	3.23	3.14	1001	1005
2	131.9	131.3	11.6	12.9	1733	1802
3	157.4	156.7	46.2	50.0	2346	2486
4	185.0	184.3	82.4	89.0	3080	3332
5	215.1	214.3	101	109	3915	4309
6	246.8	245.8	105	112	4771	5322
7	278.6	277.6	94.9	99.4	5702	6465
8	312.3	311.2	82.5	84.4	6520	7482
9	346.0	344.7	68.4	68.2	7332	8503
10	380.2	378.7	54.8	51.7	7967	9301
11	413.7	412.2	37.1	32.5	8672	10237
12	448.3	446.9	17.3	15.2	6397	7840
13	482.9	481.5	15.8	11.6	8762	10272

in the observed unphysical effects. Further, increasing the wakelength beyond 1km does not significantly improve the result. This suggests an inherent limitation of this solver.

To estimate the accuracy of the results, a comparison between the 2nd and 3rd order solution of the impedance solver is shown in Fig. 4. This comparison further substantiates the conclusion of a good accuracy up to 500 MHz. Moreover, the comparison reveals that the impedance error is due to spatial resolution, which implies that the mesh resolution for higher frequencies is insufficient. A similar behaviour is observed for the eigenmode solver.

Referring to the above comparison, the limitation of the two frequency domain solvers becomes evident. The presented 3rd order calculation of the impedance solver requires about 200 GB of RAM, with the available memory of the used machine being 256 GB. Similarly, the simulation of the eigenmode solver requires 250 GB.

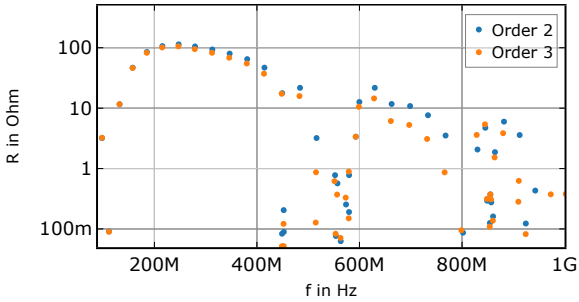

Figure 4: Convergence of shunt impedances calculated by the impedance solver with respect to order of accuracy.

Ultimately, these results emphasize the demand for further improvements in numerical methods for impedance calculations. Relying on time-consuming wakefield simulations in the time domain is not a viable option. Therefore, further improvements are necessary, in particular, for the impedance and eigenmode solvers. For the impedance solver, potential improvements could be achieved by employing techniques such as multigrid methods, domain decomposition, or concatenation methods [6].

CONCLUSION

The calculation of the IVU's shunt impedances using three different solvers up to 1.5 GHz is presented. Both the frequency domain and eigenmode solvers exhibit good accuracy up to 500 MHz, offering valuable insights into IVU properties. At higher frequencies, the accuracy of these solvers decreases, although they still reveal reasonable trends in the eigenmode spectrum and in the upper bound of the shunt impedances. Moreover, the paper provides an understanding of the simulation techniques for the given problem. Frequency domain simulations, including both eigenmode and impedance calculations, prove to be superior to time domain simulations. However, the simulation of large structures like the IVU considered in the paper still pose major challenges to numerical simulations. This stresses the demand for more efficient solvers.

REFERENCES

[1] C. G. Schroer, I. Agapov, W. Brefeld, R. Brinkmann, Y.-C. Chae, H.-C. Chao, M. Eriksson, J. Keil, X. Nuel Gavaldà, R. Röhlsberger, O. H. Seeck, M. Sprung, M. Tischer, R. Wanzenberg, and E. Weckert, "PETRA IV: The ultralow-emittance source project at DESY," *J. Synchrotron Radiat.*, vol. 25, no. 5, pp. 1277–1290, 2018. doi:10.1107/S1600577518008858

[2] T.-S. Chen, "Calculation of the parameters of ridge waveguides," *IRE Trans. Microwave Theory Tech.*, vol. 5, no. 1, pp.12–17, 1957. doi:10.1109/TMTT.1957.1125084

ISBN: 978-3-95450-231-8 ISSN: 2673-5490 doi: 10.18429/JACoW-IPAC2023-MOPM034

[3] R. Wanzenberg and T. Weiland, "Wake fields and impedances," DESY, Harmburg, Germany, Tech. Rep. DESY M-91-06, 1991.

[4] B. Gustavsen and A. Semlyen, "Rational approximation of frequency domain responses by vector fitting," *IEEE Trans. on Power Delivery*, vol. 14, no. 3, pp. 1052–1061, 1999. doi:10.1109/61.772353

[5] G. Antonini, "Spice equivalent circuits of frequency-domain responses," *IEEE Trans. Electromagn. Compat.*, vol. 45, no. 3, pp. 502–512, 2003. doi:10.1109/TEMC.2003.815528

[6] T. Flisgen, E. Gjonaj, H.-W. Glock, and A. Tsakanian, "Generalization of coupled *s*-parameter calculation to compute beam impedances in particle accelerators," *Phys. Rev. Accel. Beams*, vol. 23, p. 034601, Mar 2020. doi:10.1103/PhysRevAccelBeams.23.034601